

Article

# Optimization of the Solidification Method of High-Level Waste for Increasing the Thermal Stability of the Magnesium Potassium Phosphate Compound

Svetlana A. Kulikova \* , Sergey S. Danilov, Kseniya Yu. Belova, Anastasiya A. Rodionova and Sergey E. Vinokurov

Vernadsky Institute of Geochemistry and Analytical Chemistry of Russian Academy of Sciences, 19 Kosygin st., 119991 Moscow, Russia; danilov070992@gmail.com (S.S.D.); ksysha\_3350@mail.ru (K.Y.B.); skigirla@mail.ru (A.A.R.); vinokurov.geokhi@gmail.com (S.E.V.)

\* Correspondence: kulikova.sveta92@mail.ru; Tel.: +7-495-939-7007

Received: 18 June 2020; Accepted: 21 July 2020; Published: 23 July 2020



**Abstract:** The key task in the solidification of high-level waste (HLW) into a magnesium potassium phosphate (MPP) compound is the immobilization of mobile cesium isotopes, the activity of which provides the main contribution to the total HLW activity. In addition, the obtained compound containing heat-generating radionuclides can be significantly heated, which increases the necessity of its thermal stability. The current work is aimed at assessing the impact of various methodological approaches to HLW solidification on the thermal stability of the MPP compound, which is evaluated by the mechanical strength of the compound and its resistance to cesium leaching. High-salt surrogate HLW solution (S-HLW) used in the investigation was prepared for solidification by adding sorbents of various types binding at least 93% of  $^{137}\text{Cs}$ : ferrocyanide K-Ni (FKN), natural zeolite (NZ), synthetic zeolite Na-mordenite (MOR), and silicotungstic acid (STA). Prepared S-HLW was solidified into the MPP compound. Wollastonite (W) and NZ as fillers were added to the compound composition in the case of using FKN and STA, respectively. It was found that heat treatment up to 450 °C of the compound containing FKN and W (MPP-FKN-W) almost did not affect its compressive strength (about 12–19 MPa), and it led to a decrease of high compressive strength (40–50 MPa) of the compounds containing NZ, MOR, and STA (MPP-NZ, MPP-MOR, and MPP-STA-NZ, respectively) by an average of 2–3 times. It was shown that the differential leaching rate of  $^{137}\text{Cs}$  on the 28th day from MPP-FKN-W after heating to 250 °C was  $5.3 \times 10^{-6}$  g/(cm<sup>2</sup>·day), however, at a higher temperature, it increased by 20 and more times. The differential leaching rate of  $^{137}\text{Cs}$  from MPP-NZ, MPP-MOR, and MPP-STA-NZ had values of  $(2.9\text{--}11) \times 10^{-5}$  g/(cm<sup>2</sup>·day), while the dependence on the heat treatment temperature of the compound was negligible.

**Keywords:** magnesium potassium phosphate compound; radioactive waste; cesium; sorption; ferrocyanide K-Ni; zeolite; mordenite; silicotungstic acid; immobilization; thermal stability

## 1. Introduction

Liquid radioactive waste (LRW) of various activity levels are generated during spent nuclear fuel (SNF) reprocessing. Special attention in LRW management is paid to high-level waste (HLW) because of its high radiation hazard and biological toxicity of radionuclides. For temporary controlled storage and following final disposal, HLW must be immobilized into a solid compound that will contribute to radioecological safety for the environment. This compound should possess physical and chemical stability, including thermal stability due to its possible significant heating based on the intense heat-generating of HLW radionuclides, which is largely due to the radioactive decay of fission products, cesium isotopes ( $^{134}\text{Cs}$ ,  $^{137}\text{Cs}$ ), the activity of which provides the main contribution to the

total HLW radioactivity. The thermal stability of the compound is evaluated by its mechanical strength and resistance to leaching of radionuclides [1], mainly cesium, which is an alkali metal and, therefore, the most leached from the compound.

Previously, in a number of literary sources [2–13], it was shown that the compound based on the magnesium potassium phosphate (MPP) matrix  $\text{MgKPO}_4 \times 6\text{H}_2\text{O}$ , which is formed at room temperature and is an analogue of the natural mineral K-struvite [14], is a promising material for immobilization of various LRW types, including HLW. A key task during HLW immobilization is to ensure binding of mobile cesium isotopes in the MPP compound. To increase the hydrolytic stability of the compound, cesium isotopes should be converted to insoluble form. It is known that various sorbents are used to remove and concentrate cesium from natural and technogenic solutions.

Natural zeolites (NZ) contain clinoptilolite with a unique structure, which provides a high cation exchange ability of these sorbents and selectivity for cesium release [15–18]. Synthetic zeolite–mordenite  $\text{Na}_8\text{Al}_8\text{Si}_{40}\text{O}_{96} \times 24\text{H}_2\text{O}$  (MOR) has 12-ring cavities with a diameter of 6.5 Å or more in its structure, thus it is easy to place  $\text{Cs}_+$  ions with a radius of 3.40 Å in these cavities [19–21].

Currently, methods for binding of cesium isotopes to insoluble ferrocyanide compounds are widely used [22]. Metal hexacyanoferrates are effective sorbents for  $\text{Cs}^+$  cations as typical coordination polymers due to the comparable sizes between their structural lattices and hydrated  $\text{Cs}^+$  cations, therefore, they can selectively sorb  $\text{Cs}_+$  against other coexisting cations by ion exchange mechanism. In radiochemical technology, one of the most promising hexacyanoferrates for the selective removal of cesium is a potassium–nickel ferrocyanide with approximate composition  $\text{K}_2\text{Ni}[\text{Fe}(\text{CN})_6]$  (FKN) [23–28].

Another effective compound for the cesium isotopes binding is silicotungstic acid  $\text{H}_8[\text{Si}(\text{W}_2\text{O}_7)_6] \times n\text{H}_2\text{O}$  (STA), because  $\text{Cs}_+$  cations can enter the STA structure due to ion exchange with hydrogen, forming a water-insoluble phase [29,30]. It is known that a series of solid catalysts with STA modified with alkali metals (Li, K, Rb, and Cs) with high thermal stability and catalytic activity are synthesized [31–34].

Earlier, in some articles, the effectiveness of using NZ as a reinforcing mineral filler of the MPP compound [35,36], as well as using FKN for sorption of cesium isotopes [5,37,38] during solidification of certain LRW types, was demonstrated.

This work is aimed at studying the influence of the NZ, MOR, FKN, and STA sorbents on the efficiency of preliminary binding of  $\text{Cs}_+$  cations in the high-salt HLW solution after SNF reprocessing, as well as determination of thermal stability of the obtained MPP compounds, which is estimated from its compressive strength and stability to  $^{137}\text{Cs}$  leaching.

## 2. Materials and Methods

### 2.1. Preparation of Surrogate HLW Solution

All chemical reagents used in this study were of “analytical grade” purity.

Surrogate HLW solution (S-HLW), generated during SNF reprocessing of 1000 MW water–water energetic reactor (WWER-1000), was prepared by dissolving nitrates of the main waste components in an aqueous solution of nitric acid with a concentration of 3.0 mol/L. The metal content in the prepared S-HLW, g/L, was: La–38.1; Sr–15.0; Na–12.2; Cs–8.0; U–3.1; Mo–1.3; Zr–3.9; Cr–2.9; Ni–0.5; Fe–0.9. The content of elements in S-HLW was controlled using inductively coupled plasma atomic emission and mass spectrometry (ICP-AES and ICP-MS) (iCAP-6500 Duo and X Series2, respectively, Thermo Scientific, Waltham, MA, USA).

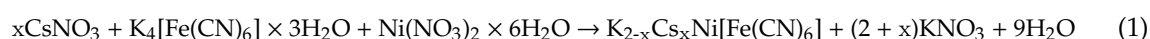
An aliquot of  $^{137}\text{Cs}$  nitrate solution was added to the prepared S-HLW; the specific activity of  $^{137}\text{Cs}$  in S-HLW was  $2.3 \times 10^7$  Bq/L.  $^{137}\text{Cs}$  content in all solutions, used in research, was determined by gamma-ray spectrometry on a spectrometer with a high-purity germanium detector GC 1020 (Canberra Ind, Meriden, CT, USA).

Preparation of S-HLW for preliminary binding of cesium isotopes and its following solidification was carried out by neutralizing it to  $\text{pH } 7.5 \pm 0.5$  by sodium hydroxide solution with a concentration

of 12.0 mol/L. Density and salt content of the prepared high-salt S-HLW were  $1.25 \pm 0.02$  g/mL and 478 g/L, respectively.

Two types of zeolites were used for preliminary binding of cesium isotopes in the prepared S-HLW: NZ of the Sokyrnytsya deposit, Transcarpathian region ("ZEO-MAX" LLC, Ramenskoye, Moscow region, Russia) and synthetic zeolite MOR (CBV 10A Na-mordenite, Zeolyst International, Conshohocken, PA, USA). Surface areas of the sorbents were 17.5 and 464.0 m<sup>2</sup>/g, respectively; particle size was not higher than 0.16 mm.

The salts of potassium hexacyanoferrate(II) trihydrate  $K_4[Fe(CN)_6] \times 3H_2O$  ("Chimmed" LLC, Moscow, Russia) and nickel(II) nitrate hexahydrate  $Ni(NO_3)_2 \times 6H_2O$  ("JSC Reahim" LLC, Moscow, Russia) were added to S-HLW in stoichiometric amount according to the reaction (1) for the binding of cesium cations in FKN.



A combination method for cesium isotopes binding was also used, which included the precipitation of cesium in S-HLW according to the reaction (2) using STA ("JSC Reahim" LLC, Moscow, Russia) followed by sorption of cesium remaining in the solution by NZ, which also was a reinforcing additive to increase the mechanical strength of the compound, as we showed earlier [36].



The obtained mixtures of S-HLW with sorbents were stirred at room temperature ( $23 \pm 2$  °C) for 30 min, which ensured the achievement of sorption equilibrium. The sorption degree *S* (%) of cesium was determined by the content of <sup>137</sup>Cs according to Equation (3), where *A*<sub>0</sub> and *A* are the initial and equilibrium activities of the radionuclide, respectively, Bq/mL.

$$S = \frac{A_0 - A}{A_0} \cdot 100 \quad (3)$$

## 2.2. Synthesis and Study of the MPP Compounds

The synthesis of the MPP compounds was carried out according to the acid–base reaction (4). For this, a dry mixture of binder MgO and KH<sub>2</sub>PO<sub>4</sub> components was added to a prepared S-HLW containing NZ or MOR zeolites, or a combined STA with NZ sorbent with preliminary bound cesium isotopes (hereinafter, the samples were designated as MPP-NZ, MPP-MOR, and MPP-STA-NZ compounds, respectively). For this, MgO precalcined at 1300 °C for 3 h (specific surface area was 6.6 m<sup>2</sup>/g) prepared according to the data in our article [39], and KH<sub>2</sub>PO<sub>4</sub> crushed to a particle size of 0.15–0.25 mm ("Rushim" LLC, Moscow, Russia) were used. The samples were prepared at the MgO:H<sub>2</sub>O (in prepared S-HLW):KH<sub>2</sub>PO<sub>4</sub> weight ratio of 1:2:3. A feature in the synthesis of the MPP compound with FKN was the use of wollastonite (W) (FW-200, Nordkalk, Pargas, Finland) in an amount of 23.3 wt % as a reinforcing additive to increase the mechanical strength of the compound (hereinafter, the sample was designated as MPP-FKN-W compound), as we showed earlier in [7,8,38].



The obtained mixtures before their setting were placed in fluoroplastic forms with cell sizes of 3 cm × 1 cm × 1 cm and stayed for at least 7 days at room temperature and atmospheric pressure for development of the compound's strength. The composition data of the synthesized MPP compounds are shown in Table 1.

The thermal stability of the obtained MPP compounds was characterized according to the mechanical strength and hydrolytic stability of the initial samples and samples after heat treatment up to 450 °C in accordance with the current requirements for solidified HLW [1]. The preliminary

removal of bound water from  $\text{MgKPO}_4 \times 6\text{H}_2\text{O}$ -based compounds was carried out at 180 °C for 6 h in a muffle furnace (SNOL 30/1300, AB UMEGA GROUP, Utena, Lithuania), as we previously showed in [38]. Then, samples of MPP-NZ, MPP-MOR, and MPP-STA-NZ compounds were kept at a maximum temperature of 450 °C according to [1], and samples of MPP-FKN-W compounds were subjected to heat treatment at various temperatures in the range of 250–450 °C for 4 h. At least three compound samples of the same composition were used in each experiment. No external changes in the compounds as a result of heat treatment were found, as is seen in the samples studied photographs (Figure 1).

**Table 1.** Composition of synthesized MPP compounds.

Compound	Sorbent (wt %)	Filler (wt %)	Solidified S-HLW (wt %)	Binders (wt %)	
				MgO	$\text{KH}_2\text{PO}_4$
MPP-FKN-W	1.5 *	23.3	34.0	10.3	30.9
MPP-NZ	25.1	-	32.1	10.7	32.1
MPP-MOR	25.1	-	32.1	10.7	32.1
MPP-STA-NZ	5.0	25.0	30.0	10.0	30.0

\* including 0.89 wt %  $\text{K}_4[\text{Fe}(\text{CN})_6] \times 3\text{H}_2\text{O}$  and 0.61 wt %  $\text{Ni}(\text{NO}_3)_2 \times 6\text{H}_2\text{O}$ .

MPP-FKN-W compound

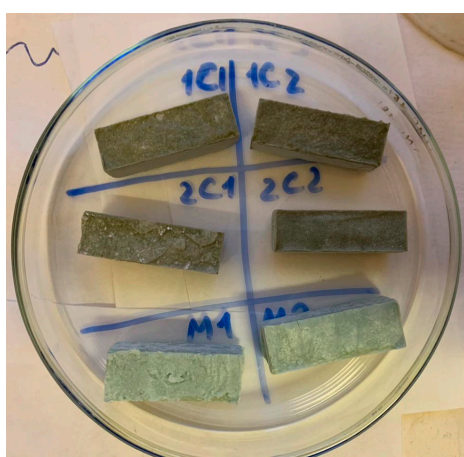


(a)



(b)

MPP-NZ and MPP-MOR compounds



(c)



(d)

**Figure 1.** Photos of initial MPP compounds (a,c) and their photos after heat treatment (b,d).

The compressive strength of the samples was determined in accordance with GOST 310.4-81 [40] when using a tensile strength-testing machine IR 5047-50 (OJSC “Tochpribor”, Moscow, Russia).

The  $^{137}\text{Cs}$  leaching rate from the initial and heat-treated monolithic MPP compounds (open geometric surface area was about  $14\text{ cm}^2$ ) was determined in accordance with GOST R 52126-2003 [41]. Before leaching, samples of the compound were immersed in ethanol for 5–7 s, then the samples were dried in air for 30 min. Next, the samples were placed in a PTFE container and double-distilled water was poured in as a leaching agent ( $\text{pH } 6.6 \pm 0.1$ , volume 100 mL), which was replaced at regular time intervals. At the set time, the samples were removed from the container, washed with double-distilled water (volume 100 mL), and combined with the leachate, and the content of  $^{137}\text{Cs}$  in the combined solution was analyzed. The calculations of the differential leaching rate  $\text{LR}_{\text{dif}}$  ( $\text{g}/(\text{cm}^2 \cdot \text{day})$ ) and cumulative fraction leached  $F$  (%) of  $^{137}\text{Cs}$  from compounds were made according to Equations (5) and (6).

From the data obtained, we calculated the effective diffusivity  $D$  ( $\text{cm}^2/\text{s}$ ), leachability index  $L$  for each leach interval, and average leachability index  $(L)_{\text{av}}$  of  $^{137}\text{Cs}$  in the MPP compounds in accordance with standard test ANSI/ANS-16.1 [42] by the Equations (7)–(9).

Leaching mechanisms of  $^{137}\text{Cs}$  from the MPP compound samples were assessed according to a de Groot and van der Sloot model [43], which can be represented as Equation (10), where values of the coefficient  $A$  (slope of the line) correspond to the following mechanisms:  $<0.35$ —surface wash-off (or a depletion if it is found in the middle or at the end of the test);  $0.35$ – $0.65$ —diffusion transport;  $>0.65$ —surface dissolution [44]. The calculation of  $B_i$  was carried out according to Equation (11).

$$\text{LR}_{\text{dif}} = \frac{A_n}{A_0 \cdot S \cdot \Delta t_n} \quad (5)$$

$$F = \frac{\sum A_n}{A_0} \cdot 100 \quad (6)$$

$$D = \pi \left( \frac{A_0/A_n}{(\Delta t)_n} \right)^2 \cdot \left( \frac{V_c}{S} \right)^2 \quad (7)$$

$$L = -\log(D) \quad (8)$$

$$(L)_{\text{av}} = \frac{1}{n} \sum_1^n (L)_n \quad (9)$$

$$\log(B_i) = A \log(t_n) + \text{const} \quad (10)$$

$$B_i = A_n \cdot \frac{V}{S} \cdot \frac{\sqrt{t_n}}{(\sqrt{t_n} - \sqrt{t_{n-1}})} \quad (11)$$

where  $A_n$ —activity of  $^{137}\text{Cs}$  leached for a given time interval, Bq;  $A_0$ —specific activity of  $^{137}\text{Cs}$  in the initial sample, Bq/g;  $S$ —the area of the open geometric surface of the sample, contacting with water,  $\text{cm}^2$ ;  $\Delta t_n$ —duration of the  $n$ -th leaching period between shifts of contact solution, day;  $B_i$ —the total release of  $^{137}\text{Cs}$  from the sample during the time contact with water,  $\text{mg}/\text{m}^2$ ;  $V$ —the volume of the contact solution, L;  $V_c$ —volume of compound,  $\text{cm}^3$ ;  $t_n$  and  $t_{n-1}$ —the total contact time for the period  $n$  and before the beginning of the period  $n$ , respectively, days.

### 3. Results and Discussion

The maximum experimental sorption degree of  $^{137}\text{Cs}$  by various sorbents in the prepared S-HLW was determined (Table 2). It was established that  $^{137}\text{Cs}$  was quantitatively sorbed in the case of MPP-FKN-W and MPP-STA-NZ: 99.5 and 99.1%, respectively (and 97% of  $^{137}\text{Cs}$  was associated with the introduction of STA in the case of MPP-STA-NZ). The sorption degree of  $^{137}\text{Cs}$  by zeolites for MPP-NZ and MPP-MOR samples achieved 93.0 and 98.5%, respectively. The results of studying the thermal stability of the prepared samples of the MPP compounds, namely, the determination of the compressive strength and resistance to  $^{137}\text{Cs}$  leaching, are given below.

**Table 2.** The results of  $^{137}\text{Cs}$  sorption by various sorbents in the prepared S-HLW.

Sorbent	$^{137}\text{Cs}$ Sorption Degree (%)
FKN	99.5
NZ	93.0
MOR	98.5
STA/NZ	97.0/99.1

### 3.1. Thermal Stability of MPP-FKN-W Compound

The obtained data on the compressive strength of MPP-FKN-W compound samples depending on the temperature of their heat treatment are presented in Figure 2. It was established that heating of the compound in the range of 180 to 450 °C does not lead to a decrease in its compressive strength, which is about 12–19 MPa, which corresponds to the strength of vitrified HLW [1] (not less than 9 MPa). At the same time, a decrease of the compressive strength of the compound from 18 to 12 MPa after heat treatment at 180 °C was established, which is obviously due to an increase of the compound porosity because of removal of bound water from the  $\text{MgKPO}_4 \times 6\text{H}_2\text{O}$  composition, whereas with a further increase of the heat treatment temperature to 450 °C, the strength of the compound grows to values of 15–19 MPa, probably due to the beginning of the sintering process of single compound particles.

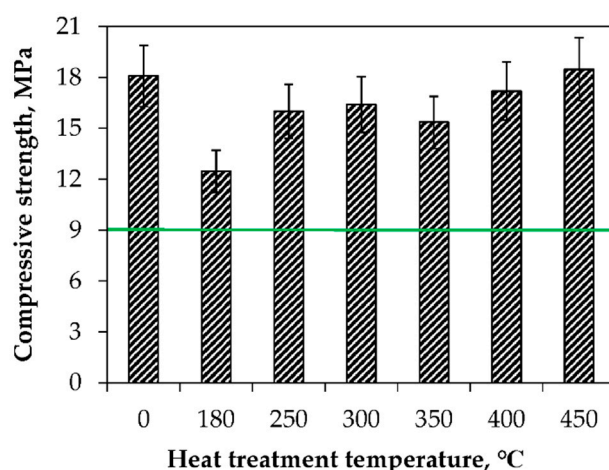


**Figure 2.** Compressive strength of MPP-FKN-W compound samples in dependence on the temperature of their heat treatment (green line is the lower limit of the compressive strength requirements for vitrified HLW [1]).

The dependence of the differential leaching rate of  $^{137}\text{Cs}$  from MPP-FKN-W compound samples is shown in Figure 3, and the  $^{137}\text{Cs}$  leaching data from the samples in contact with water are given in Table 3. It was found that MPP-FKN-W compound retains high resistance to  $^{137}\text{Cs}$  leaching to 250 °C. So, the  $^{137}\text{Cs}$  leaching rate from MPP-FKN-W compound, heated to 250 °C on the 28<sup>th</sup> day, is  $5.3 \times 10^{-6}$  g/(cm<sup>2</sup>·day), which corresponds to the requirements for aluminophosphate glass (not more than  $1.0 \times 10^{-5}$  g/(cm<sup>2</sup>·day)) [1], which are usually achieved on days 14–21 of the standard test [41].

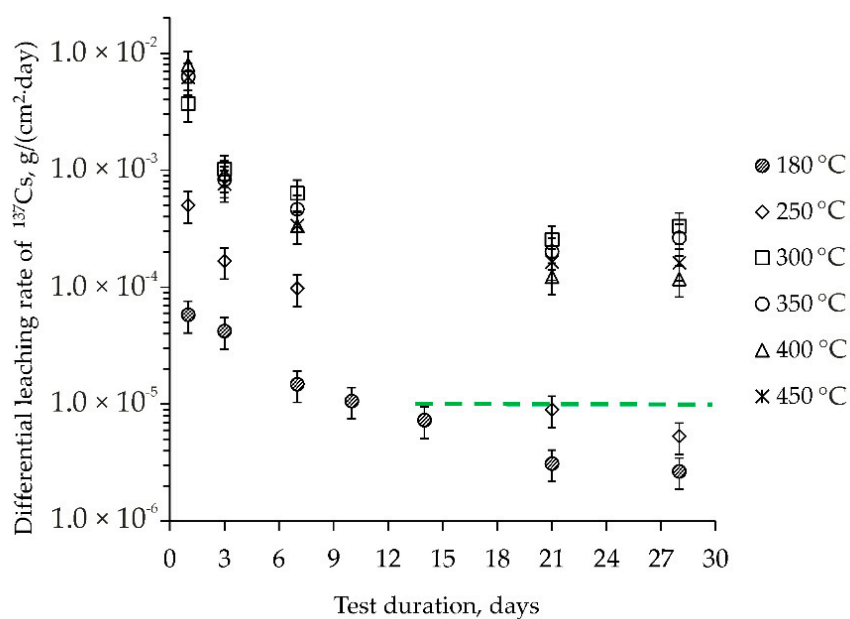
At the same time, as the temperature increases to  $\geq 300$  °C, the  $^{137}\text{Cs}$  leaching rate increases to  $(1.2\text{--}3.3) \times 10^{-4}$  g/(cm<sup>2</sup>·day), and the cumulative fraction leached of  $^{137}\text{Cs}$  from MPP-FKN-W compound after their heat treatment at  $\geq 300$  °C is about 5% (Table 3), which is an order of magnitude higher than at 250 °C. Obviously, at the temperature of  $\geq 300$  °C, cesium immobilized in MPP-FKN-W compound partially transforms into composition of much more soluble compounds than FKN. It is in accordance with the conditions of thermal decomposition of FKN in [45], where it was shown that thermal decomposition of CN groups occurs at temperature above 250 °C, the intermediate cyanides  $\text{K}_3\text{Fe}(\text{CN})_6$  and/or  $\text{K}_3\text{Ni}(\text{CN})_6$  are formed in the temperature range from 280 to 330 °C,  $\text{K}_2\text{CO}_3$ ,  $\text{NiO}$ ,

and  $\text{NiFe}_2\text{O}_4$  are formed from 250 to 400 °C, and with a further increase in temperature above 450 °C, the intermediate cyanides will decompose.

The  $(L)_{av}$  values of  $^{137}\text{Cs}$  from MPP-FKN-W compound are 10–14 (Table 3), which meet the leachability requirements for the waste form to be accepted at the radioactive waste repository (minimum  $(L)_{av}$  is 6.0) according to the U.S. Nuclear Regulatory Commission [46], and approach the  $(L)_{av}$  value of cesium from borosilicate glass  $(L)_{av} = 16.93$  [47]. It was noted that heat treatment of the compound above 250 °C decreased the  $(L)_{av}$  of  $^{137}\text{Cs}$  from the compound ( $(L)_{av}$  is about 10.0) as the F increased (Table 3).

Figure 4 illustrates the effect of heat treatment on the  $^{137}\text{Cs}$  leaching mechanism on the example of MPP-FKN-W compounds heated to 180 and 450 °C. So, for MPP-FKN-W compound heated to 180 °C, the  $^{137}\text{Cs}$  leaching occurs due to the release of weakly bound cesium at dissolution of the surface compound layer (coefficient  $A = 1.12$  in Equation (10)) in the first three days of contact of the compound's with water, and then due to the gradual depletion of the surface layer of the compound ( $A = -0.19$ ). Thus, the compound exhibits high hydrolytic stability, in which  $^{137}\text{Cs}$  remains quantitatively immobilized in the compound.

Moreover, in the case of MPP-FKN-W compound heated to 450 °C, a significant amount of  $^{137}\text{Cs}$  has already been leached at the first day of the compound's contact with water when the obtained readily soluble forms of  $^{137}\text{Cs}$  are dissolved, then depletion of the surface layer of the compound occurs for up to seven days ( $A = -0.25$ ), and after that, diffusion from the inner layers of the compound becomes the main leaching mechanism of  $^{137}\text{Cs}$  ( $A = 0.49$ ).

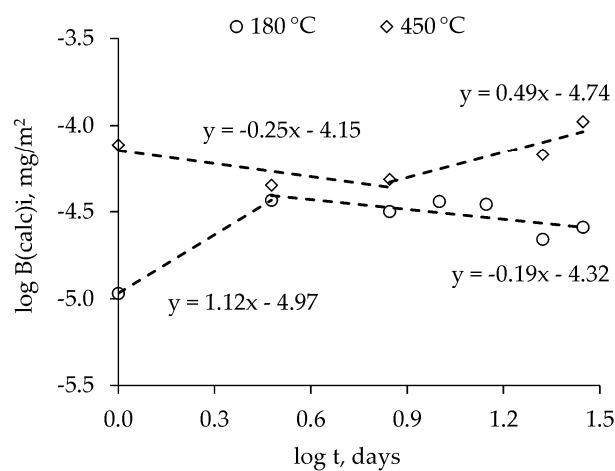


**Figure 3.** Kinetic curves of the  $^{137}\text{Cs}$  leaching rate from MPP-FKN-W compound samples in dependence on the temperature of their heat treatment (green line is the upper limit of the  $^{137}\text{Cs}$  leaching rate requirements for vitrified HLW [1]).

Thus, the obtained data on the thermal stability of MPP-FKN-W compound allow the consideration of this material as an effective alternative even to an industrial glass-like compound for solidification of HLW, but only under the condition that the heating of the compound does not achieve temperatures above 250 °C. At the same time, the HLW solidification technology using MPP-FKN-W compound looks preferable to vitrification, since it does not require expensive high-temperature melting equipment and gas cleaning systems, and also eliminates the huge radioecological problem of decommissioning this equipment.

**Table 3.** Leaching data of  $^{137}\text{Cs}$  from MPP-FKN-W compound.

Heat Treatment Temperature (°C)	Test Duration (days)	F (%)	D ( $\text{cm}^2/\text{s}$ )	L	(L) <sub>av</sub>
180	1	0.01	$1.1 \times 10^{-14}$	14.0	14.1
	3	0.03	$4.2 \times 10^{-14}$	13.4	
	7	0.04	$1.3 \times 10^{-14}$	13.9	
	10	0.04	$1.2 \times 10^{-14}$	13.9	
	14	0.05	$8.0 \times 10^{-15}$	14.1	
	21	0.05	$2.1 \times 10^{-15}$	14.7	
	28	0.05	$2.2 \times 10^{-15}$	14.7	
250	1	0.18	$1.4 \times 10^{-12}$	11.8	12.4
	3	0.31	$1.2 \times 10^{-12}$	11.9	
	7	0.45	$1.0 \times 10^{-12}$	12.0	
	21	0.68	$5.8 \times 10^{-13}$	12.2	
	28	0.69	$1.6 \times 10^{-14}$	13.8	
300	1	1.33	$7.4 \times 10^{-11}$	10.1	10.4
	3	2.06	$4.2 \times 10^{-11}$	10.4	
	7	2.98	$4.2 \times 10^{-11}$	10.4	
	21	4.27	$1.9 \times 10^{-11}$	10.7	
	28	5.10	$5.8 \times 10^{-11}$	10.2	
350	1	2.19	$2.0 \times 10^{-10}$	9.7	10.5
	3	2.77	$2.6 \times 10^{-11}$	10.6	
	7	3.41	$2.1 \times 10^{-11}$	10.7	
	21	4.39	$1.1 \times 10^{-11}$	11.0	
	28	5.03	$3.4 \times 10^{-11}$	10.5	
400	1	2.63	$2.9 \times 10^{-10}$	9.5	10.7
	3	3.26	$3.1 \times 10^{-11}$	10.5	
	7	3.71	$1.0 \times 10^{-11}$	11.0	
	21	4.30	$3.8 \times 10^{-12}$	11.4	
	28	4.58	$6.5 \times 10^{-12}$	11.2	
450	1	2.28	$2.2 \times 10^{-10}$	9.7	10.6
	3	2.84	$2.4 \times 10^{-11}$	10.6	
	7	3.33	$1.2 \times 10^{-11}$	10.9	
	21	4.17	$7.9 \times 10^{-12}$	11.1	
	28	4.59	$1.4 \times 10^{-11}$	10.8	

**Figure 4.** Logarithmic dependence of the  $^{137}\text{Cs}$  release from MPP-FKN-W compound samples on contact time with water.

### 3.2. Thermal Stability of MPP-NZ, MPP-MOR, and MPP-STA-NZ Compounds

The compressive strength of MPP-NZ, MPP-MOR, and MPP-STA-NZ compound samples after seven days after preparation is shown in Figure 5. Also for comparison, Figure 5 shows the strength of the blank MPP compound obtained after solidification of S-HLW and not containing sorbents. From these data, it can be seen that the strength of the blank MPP compound after heat treatment at 450 °C decreases by 3 times, from 12–14 to 3–5 MPa, which does not satisfy the requirements (at least 9 MPa) [1]. At the same time, it was shown that the addition of sorbents and mineral fillers increases the compressive strength of the initial compounds up to 40–50 MPa, regardless of the sorbent used (Figure 5). There was a tendency toward a decrease in the compressive strength of the samples after heat treatment at 180 and 450 °C (Figure 5), however, the required compressive strength remains and is about 10–25 MPa.

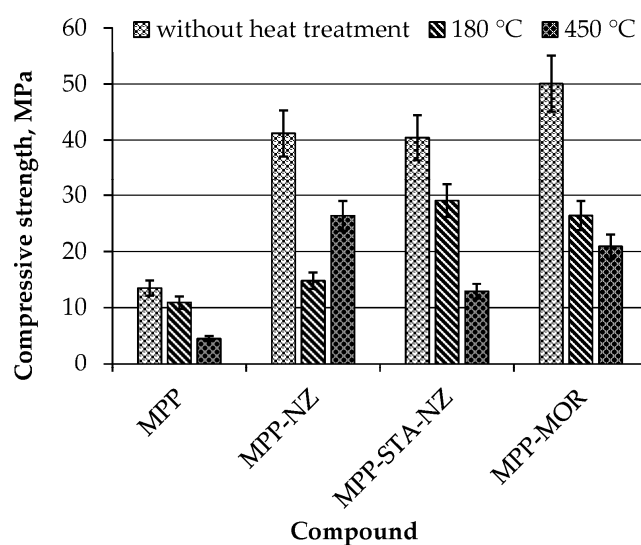
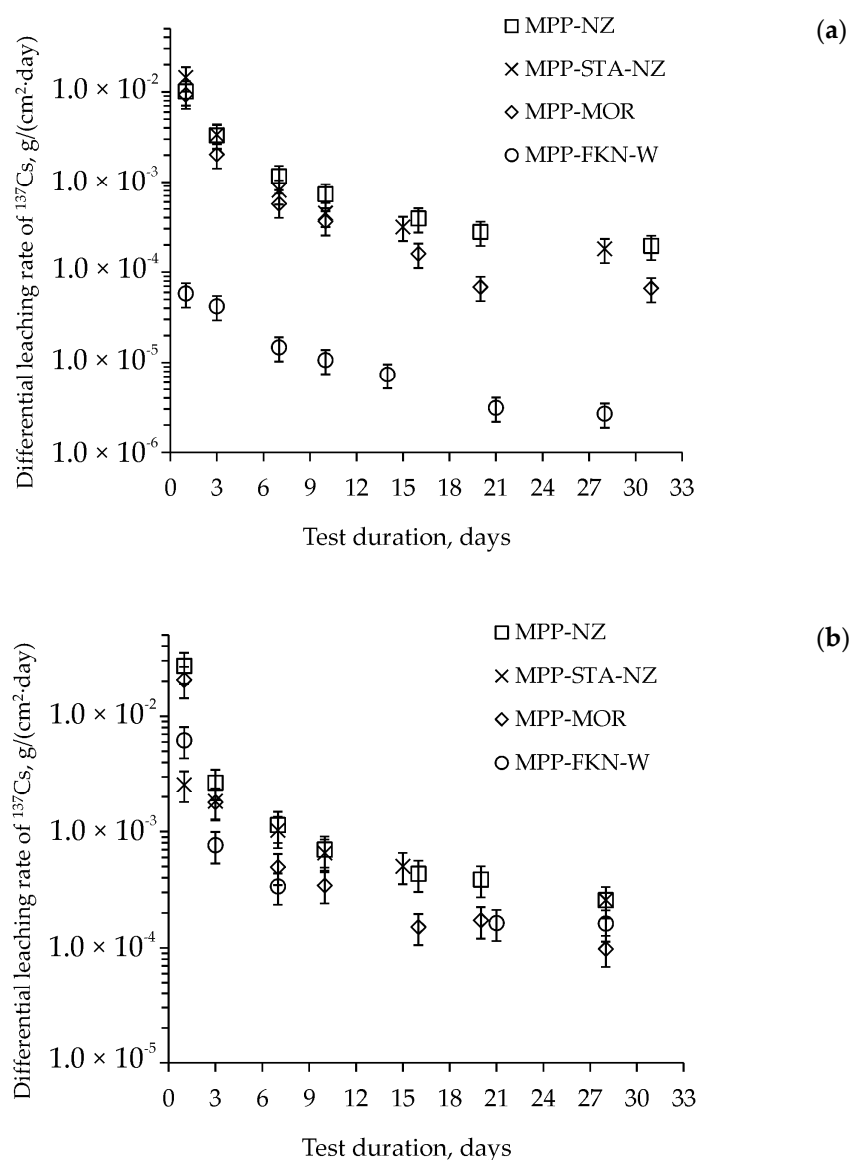


Figure 5. Compressive strength of the MPP compounds.

The results of studying the hydrolytic stability of MPP-NZ, MPP-MOR, and MPP-STA-NZ compounds after heat treatment to 180 and 450 °C are presented in Figure 6a,b, respectively; for comparison, Figure 6 is also supplemented with relevant data for MPP-FKN-W compound. It was shown that the  $^{137}\text{Cs}$  leaching kinetics from MPP-NZ, MPP-MOR, and MPP-STA-NZ compounds, containing various sorbents, have a generally similar character, with small dependency on the heat treatment temperature. At the same time, the  $^{137}\text{Cs}$  leaching rate from these compounds after heat treatment up to 180 °C is 20–100 times higher than that in the case of MPP-FKN-W compound (Figure 6a). On the other hand, increasing the heat treatment temperature from 180 to 450 °C (Figure 6a,b, respectively) does not affect the  $^{137}\text{Cs}$  leaching rate from MPP-NZ, MPP-MOR, and MPP-STA-NZ compounds so critically as for MPP-FKN-W compound (Figure 3). In this case, the  $^{137}\text{Cs}$  leaching rate from all compounds under study after heat treatment up to 450 °C is almost equalized (Figure 6b), being approximately  $(1\text{--}3) \times 10^{-4} \text{ g}/(\text{cm}^2 \cdot \text{day})$  after a month of testing [41].

The data of long-term (up to 91 days)  $^{137}\text{Cs}$  leaching from MPP-NZ, MPP-MOR, and MPP-STA-NZ compounds are summarized in Table 4. The differential leaching rate of cesium from compounds with long-term leaching stabilizes in the range  $(2.9\text{--}11) \times 10^{-5} \text{ g}/(\text{cm}^2 \cdot \text{day})$  with a corresponding  $(L)_{\text{av}}$  of about 10–11 (Table 4). The cumulative fractions leached of  $^{137}\text{Cs}$  from MPP-NZ and MPP-MOR compounds after heat treatment at 450 °C (Table 4) are 19.40 and 10.00%, respectively, which is 1.7 times higher than the values for these samples heat-treated at 180 °C (Table 4). If we take into account that the amount of free (unadsorbed) cesium in S-HLW is 7.0 and 1.5% (from data of Table 2) during the synthesis of these compounds, then we can recognize that these compounds show almost the same resistance to  $^{137}\text{Cs}$  leaching.



**Figure 6.** Kinetic curves of the  $^{137}\text{Cs}$  leaching rate from the compounds after heat treatment at 180 (a) and 450 °C (b).

The leaching mechanisms of  $^{137}\text{Cs}$  from MPP-NZ and MPP-MOR (Figure 7a,c, respectively) during long-term contact with water in general are similar with each other except for the initial experiment stage, which obviously provides the main contribution to increasing the cumulative fraction leached of  $^{137}\text{Cs}$  after heat treatment of these compounds at 450 °C. In this case, the thermal stability up to 450 °C of MPP-STA-NZ compound is not getting worse: the cumulative fraction leached of  $^{137}\text{Cs}$  even decreases from 9.35 to 7.03% (Table 4), which is also associated with a difference in the leaching mechanism of  $^{137}\text{Cs}$  at the first day of the compound contact with water. In general, when comparing the data in Tables 3 and 4, it should be concluded that MPP-FKN-W compound has a higher thermal stability among all the compounds under study.

Table 4. Leaching data of  $^{137}\text{Cs}$  from the MPP compounds.

Compound	Heat Treatment Temperature ( $^{\circ}\text{C}$ )	Test Duration (Days)	F (%)	D ( $\text{cm}^2/\text{s}$ )	L	(L) <sub>av</sub>	
MPP-NZ	180	1	3.48	$5.1 \times 10^{-10}$	9.3	10.3	
		3	5.77	$4.1 \times 10^{-10}$	9.4		
		7	7.37	$1.3 \times 10^{-10}$	9.9		
		10	8.13	$8.9 \times 10^{-11}$	10.1		
		16	8.94	$3.9 \times 10^{-11}$	10.4		
		20	9.32	$2.8 \times 10^{-11}$	10.6		
		31	10.06	$1.9 \times 10^{-11}$	10.7		
		59	10.75	$4.5 \times 10^{-12}$	11.3		
		91	11.34	$4.2 \times 10^{-12}$	11.4		
	450	1	9.88	$4.1 \times 10^{-9}$	8.4	10.0	
		3	11.83	$3.0 \times 10^{-10}$	9.5		
		7	13.50	$1.4 \times 10^{-10}$	9.9		
		10	14.27	$9.2 \times 10^{-11}$	10.0		
		16	15.22	$5.4 \times 10^{-11}$	10.3		
		20	15.78	$6.0 \times 10^{-11}$	10.2		
		31	16.82	$3.7 \times 10^{-11}$	10.4		
		59	18.17	$1.7 \times 10^{-11}$	10.8		
		91	19.40	$1.8 \times 10^{-11}$	10.7		
MPP-STA-NZ	180	1	4.23	$7.5 \times 10^{-10}$	9.1	10.7	
		3	6.22	$3.1 \times 10^{-10}$	9.5		
		7	7.17	$4.5 \times 10^{-11}$	10.3		
		10	7.56	$2.5 \times 10^{-11}$	10.6		
		15	8.02	$1.8 \times 10^{-11}$	10.8		
		28	8.71	$9.8 \times 10^{-12}$	11.0		
		59	9.08	$9.8 \times 10^{-13}$	12.0		
		91	9.35	$9.0 \times 10^{-13}$	12.0		
		450	1	0.78	$2.5 \times 10^{-11}$		10.6
	3		1.88	$9.5 \times 10^{-11}$	10.0		
	7		3.13	$7.7 \times 10^{-11}$	10.1		
	10		3.72	$5.6 \times 10^{-11}$	10.3		
	15		4.49	$4.8 \times 10^{-11}$	10.3		
	28		5.49	$2.1 \times 10^{-11}$	10.7		
	59		6.35	$5.3 \times 10^{-12}$	11.3		
	91		7.03	$5.6 \times 10^{-12}$	11.3		
	MPP-MOR		180	1	2.83	$3.3 \times 10^{-10}$	9.5
		3		4.06	$1.2 \times 10^{-10}$	9.9	
7		4.75		$2.4 \times 10^{-11}$	10.6		
10		5.08		$1.7 \times 10^{-11}$	10.8		
16		5.37		$5.0 \times 10^{-12}$	11.3		
20		5.46		$1.3 \times 10^{-12}$	11.9		
31		5.68		$1.7 \times 10^{-12}$	11.8		
59		6.18		$2.3 \times 10^{-12}$	11.6		
91		6.79		$4.5 \times 10^{-12}$	11.3		
450		1	6.25	$1.6 \times 10^{-9}$	8.8	10.8	
		3	7.34	$9.3 \times 10^{-11}$	10.0		
		7	7.95	$1.8 \times 10^{-11}$	10.7		
		10	8.26	$1.6 \times 10^{-11}$	10.8		
		16	8.54	$4.5 \times 10^{-12}$	11.3		
		20	8.75	$8.3 \times 10^{-12}$	11.1		
		31	9.08	$3.8 \times 10^{-12}$	11.4		
		59	9.58	$2.3 \times 10^{-12}$	11.6		
		91	10.00	$2.1 \times 10^{-12}$	11.7		

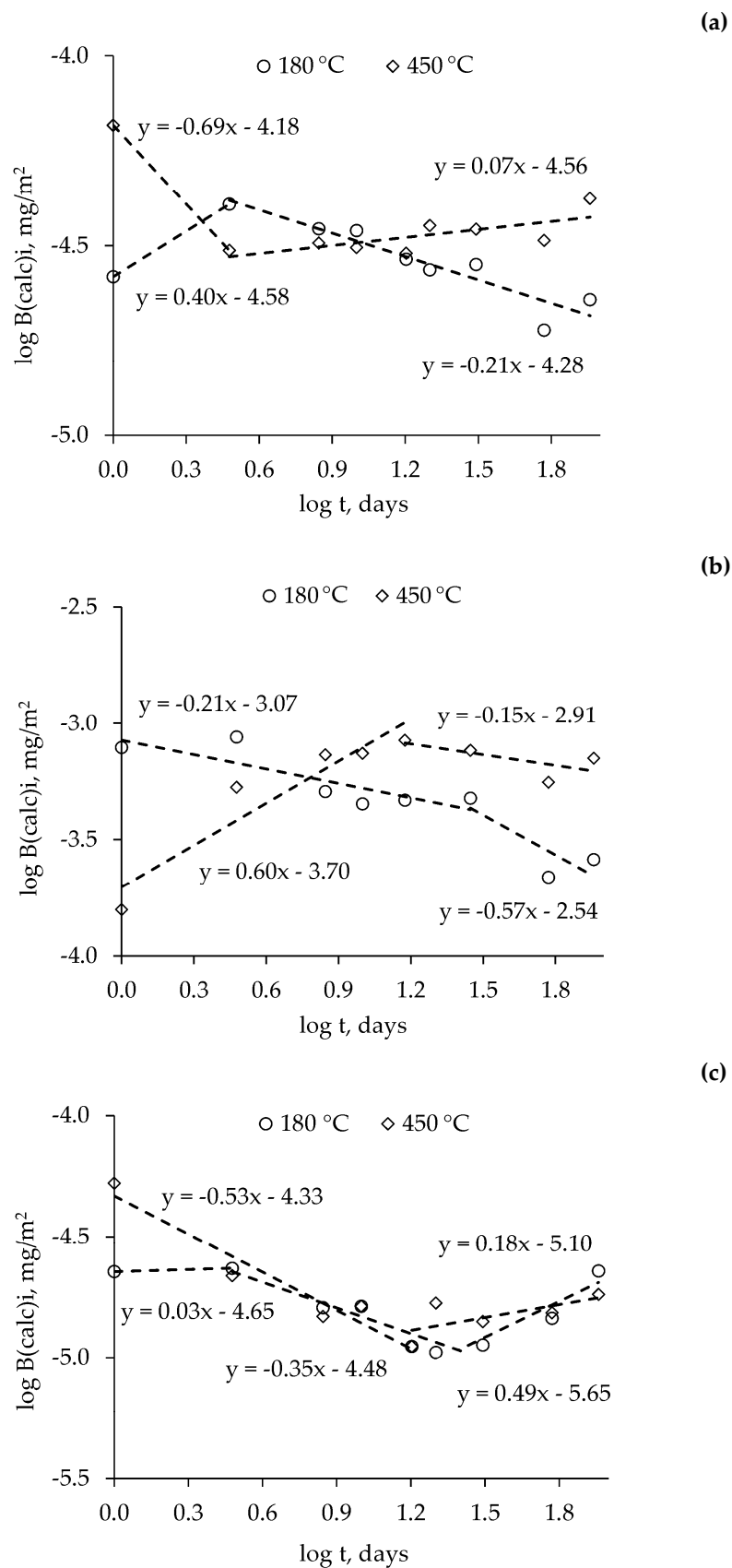


**Figure 7.** Logarithmic dependence of the <sup>137</sup>Cs release from MPP-NZ (a), MPP-STA-NZ (b), and MPP-MOR (c) compounds on contact time with water.

#### 4. Conclusions

As a result of the studies, the thermal stability of the MPP compounds containing sorbents of various nature was determined. It has been established that MPP-FKN-W compound is an effective alternative to an industrial glass-like compound for HLW solidification if the compound heating due to the heat-generating of HLW radionuclides does not achieve temperatures above 250 °C, since below this temperature, the compound retains high hydrolytic stability to <sup>137</sup>Cs leaching. At the same time, it was shown that the thermal stability of MPP-NZ, MPP-MOR, and MPP-STA-NZ compounds does not decrease even at higher heating temperatures (up to 450 °C), however, their resistance to <sup>137</sup>Cs leaching is lower in comparison with glass, therefore, these compounds can be considered for the HLW solidification after removal of the cesium-containing fraction from HLW.

**Author Contributions:** Conceptualization, S.A.K. and S.E.V.; methodology, S.A.K. and S.S.D.; validation, S.A.K., S.S.D., and S.E.V.; formal analysis, S.A.K., S.S.D., K.Y.B., and A.A.R.; investigation, S.A.K., S.S.D., K.Y.B., and A.A.R.; writing—original draft preparation, S.A.K.; writing—review and editing, S.E.V.; visualization, S.A.K. and S.E.V.; supervision, S.E.V.; project administration, S.E.V.; funding acquisition, S.E.V. All authors have read and agreed to the published version of the manuscript.

**Funding:** Compounds were prepared as part of the work on contract No 24-19-997/13914/1195 with FSUE “MCC”, and the research of the hydrolytic stability of the compounds was funded by Russian Science Foundation, grant No 16-13-10539.

**Conflicts of Interest:** The authors declare no conflict of interest. The funders had no role in the design of the study; in the collection, analyses, or interpretation of data; in the writing of the manuscript, or in the decision to publish the results.

#### References

1. Federal Norms and Rules in the Field of Atomic Energy Use. In “Collection, Processing, Storage and Conditioning of Liquid Radioactive Waste. Safety Requirements” (NP-019-15); Rostekhnadzor: Moscow, Russia, 2015; pp. 1–22.
2. Wagh, A.S. *Chemically Bonded Phosphate Ceramics; Chemically Bonded Phosphate Ceramics: Twenty-First Century Materials with Diverse Applications*, 2nd ed.; Elsevier: Amsterdam, The Netherlands, 2016; pp. 1–422, ISBN 978-0-08-100380-0.
3. Wagh, A.; Străin, R.; Jeong, S.; Reed, D.; Krause, T.; Singh, D. Stabilization of Rocky Flats Pu-contaminated ash within chemically bonded phosphate ceramics. *J. Nucl. Mater.* **1999**, *265*, 295–307. [[CrossRef](#)]
4. Singh, D.; Mandalika, V.; Parulekar, S.J.; Wagh, A. Magnesium potassium phosphate ceramic for <sup>99</sup>Tc immobilization. *J. Nucl. Mater.* **2006**, *348*, 272–282. [[CrossRef](#)]
5. Vinokurov, S.; Kulyako, Y.; Slyuntchev, O.; Rovny, S.; Myasoedov, B. Low-temperature immobilization of actinides and other components of high-level waste in magnesium potassium phosphate matrices. *J. Nucl. Mater.* **2009**, *385*, 189–192. [[CrossRef](#)]
6. Vinokurov, S.E.; Kulikova, S.A.; Myasoedov, B.F. Magnesium Potassium Phosphate Compound for Immobilization of Radioactive Waste Containing Actinide and Rare Earth Elements. *Materials* **2018**, *11*, 976. [[CrossRef](#)] [[PubMed](#)]
7. Vinokurov, S.E.; Kulikova, S.A.; Myasoedov, B.F. Hydrolytic and thermal stability of magnesium potassium phosphate compound for immobilization of high level waste. *J. Radioanal. Nucl. Chem.* **2018**, *318*, 2401–2405. [[CrossRef](#)]
8. Vinokurov, S.E.; Kulikova, S.A.; Myasoedov, B.F. Solidification of high level waste using magnesium potassium phosphate compound. *Nucl. Eng. Technol.* **2019**, *51*, 755–760. [[CrossRef](#)]
9. Dmitrieva, A.V.; Kalenova, M.Y.; Kulikova, S.A.; Kuznetsov, I.V.; Koshcheev, A.M.; Vinokurov, S.E. Magnesium-Potassium Phosphate Matrix for Immobilization of <sup>14</sup>C. *Russ. J. Appl. Chem.* **2018**, *91*, 641–646. [[CrossRef](#)]
10. Kulikova, S.A.; Belova, K.Y.; Tyupina, E.A.; Vinokurov, S.E. Conditioning of Spent Electrolyte Surrogate LiCl-KCl-CsCl Using Magnesium Potassium Phosphate Compound. *Energies* **2020**, *13*, 1963. [[CrossRef](#)]
11. Shkuropatenko, V.A. High level wastes immobilization in ceramic and hydrated phosphate matrix. *East Eur. J. Phys.* **2016**, *3*, 49–60. [[CrossRef](#)]

12. Zhenyu, L.; Hongtao, W.; Yang, H.; Tao, Y.; Zhongyuan, L.; Shuzhen, L.; Haibin, Z. Rapid solidification of Highly Loaded High-Level Liquid Wastes with magnesium phosphate cement. *Ceram. Int.* **2019**, *45*, 5050–5057. [[CrossRef](#)]
13. Tao, Y.; Zhenyu, L.; Chunrong, R.; Yuanyuan, W.; Zhichao, H.; Xin, H.; Jie, W.; Mengliang, L.; Qiubai, D.; Khan, K.; et al. Study on solidification properties of chemically bonded phosphate ceramics for cesium radionuclides. *Ceram. Int.* **2020**, *46*, 14964–14971. [[CrossRef](#)]
14. Graeser, S.; Postl, W.; Bojar, H.-P.B.; Armbruster, T.; Raber, T.; Ettinger, K.; Walter, F.; Berlepsch, P. Struvite-(K),  $\text{KMgPO}_4\cdot\text{H}_2\text{O}$ , the potassium equivalent of struvite a new mineral. *Eur. J. Mineral.* **2008**, *20*, 629–633. [[CrossRef](#)]
15. Shahwan, T.; Akar, D.; Eroglu, A.E. Physicochemical characterization of the retardation of aqueous  $\text{Cs}^+$  ions by natural kaolinite and clinoptilolite minerals. *J. Colloid Interface Sci.* **2005**, *285*, 9–17. [[CrossRef](#)] [[PubMed](#)]
16. Belousov, P.; Semenkova, A.; Egorova, T.B.; Romanchuk, A.Y.; Zakusin, S.; Dorzhieva, O.; Tyupina, E.; Izosimova, Y.; Tolpeshta, I.; Chernov, M.; et al. Cesium Sorption and Desorption on Glauconite, Bentonite, Zeolite and Diatomite. *Minerals* **2019**, *9*, 625. [[CrossRef](#)]
17. Abusafa, A.; Yücel, H. Removal of  $^{137}\text{Cs}$  from aqueous solutions using different cationic forms of a natural zeolite: Clinoptilolite. *Sep. Purif. Technol.* **2002**, *28*, 103–116. [[CrossRef](#)]
18. Johan, E.; Yamada, T.; Munthali, M.W.; Kabwadza-Corner, P.; Aono, H.; Matsue, N. Natural Zeolites as Potential Materials for Decontamination of Radioactive Cesium. *Procedia Environ. Sci.* **2015**, *28*, 52–56. [[CrossRef](#)]
19. Borai, E.H.; Harjula, R.; Malinen, L.; Paajanen, A. Efficient removal of cesium from low-level radioactive liquid waste using natural and impregnated zeolite minerals. *J. Hazard. Mater.* **2009**, *172*, 416–422. [[CrossRef](#)]
20. Aono, H.; Kunitomo, T.; Takahashi, R.; Itagaki, Y.; Johan, E.; Matsue, N.  $\text{Cs}^+$  decontamination properties of mordenites and composite materials synthesized from coal fly ash and rice husk ash. *J. Asian Ceram. Soc.* **2018**, *6*, 213–221. [[CrossRef](#)]
21. Aono, H.; Takeuchi, Y.; Itagaki, Y.; Johan, E. Synthesis of chabazite and merlinoite for  $\text{Cs}^+$  adsorption and immobilization properties by heat-treatment. *Solid State Sci.* **2020**, *100*, 106094. [[CrossRef](#)]
22. Wang, J.; Zhuang, S.; Liu, Y. Metal hexacyanoferrates-based adsorbents for cesium removal. *Coord. Chem. Rev.* **2018**, *374*, 430–438. [[CrossRef](#)]
23. Mimura, H.; Lehto, J.; Harjula, R. Ion Exchange of Cesium on Potassium Nickel Hexacyanoferrate (II)s. *J. Nucl. Sci. Technol.* **1997**, *34*, 484–489. [[CrossRef](#)]
24. Michel, C.; Barre, Y.; De Dieuleveult, C.; Grandjean, A.; De Windt, L. Cs ion exchange by a potassium nickel hexacyanoferrate loaded on a granular support. *Chem. Eng. Sci.* **2015**, *137*, 904–913. [[CrossRef](#)]
25. Tachikawa, H.; Haga, K.; Yamada, K. Mechanism of  $\text{K}^+$ ,  $\text{Cs}^+$  ion exchange in nickel ferrocyanide: A density functional theory study. *Comput. Theor. Chem.* **2017**, *1115*, 175–178. [[CrossRef](#)]
26. Martin, I.; Patapy, C.; Boher, C.; Cyr, M. Investigation of caesium retention by potassium nickel hexacyanoferrate (II) in different pH conditions and potential effect on the selection of storage matrix. *J. Nucl. Mater.* **2019**, *526*, 151764. [[CrossRef](#)]
27. Avramenko, V.; Bratskaya, S.; Zheleznov, V.; Sheveleva, I.; Voitenko, O.; Sergienko, V. Colloid stable sorbents for cesium removal: Preparation and application of latex particles functionalized with transition metals ferrocyanides. *J. Hazard. Mater.* **2011**, *186*, 1343–1350. [[CrossRef](#)]
28. Voronina, A.; Noskova, A.Y.; Semenishchev, V.; Gupta, D. Decontamination of seawater from  $^{137}\text{Cs}$  and  $^{90}\text{Sr}$  radionuclides using inorganic sorbents. *J. Environ. Radioact.* **2020**, *217*, 106210. [[CrossRef](#)]
29. Oh, S.-Y.; Kawai, K.; Kawamura, G.; Muto, H.; Matsuda, A. Characterization of mechanochemically synthesized  $\text{MHSO}_4\text{-H}_4\text{SiW}_{12}\text{O}_{40}$  composites ( $\text{M} = \text{K}, \text{NH}_4, \text{Cs}$ ). *Mater. Res. Bull.* **2012**, *47*, 2931–2935. [[CrossRef](#)]
30. Pesaresi, L.; Brown, D.; Lee, A.; Montero, J.; Williams, H.; Wilson, K. Cs-doped  $\text{H}_4\text{SiW}_{12}\text{O}_{40}$  catalysts for biodiesel applications. *Appl. Catal. A Gen.* **2009**, *360*, 50–58. [[CrossRef](#)]
31. Zhu, S.; Gao, X.; Zhu, Y.; Xiang, X.; Hu, C.; Li, Y. Alkaline metals modified  $\text{Pt-H}_4\text{SiW}_{12}\text{O}_{40}\text{ZrO}_2$  catalysts for the selective hydrogenolysis of glycerol to 1,3-propanediol. *Appl. Catal. B Environ.* **2013**, *140*, 60–67. [[CrossRef](#)]
32. Sawant, D.P.; Vinu, A.; Mirajkar, S.; Lefebvre, F.; Ariga, K.; Anandan, S.; Mori, T.; Nishimura, C.; Halligudi, S. Silicotungstic acid/zirconia immobilized on SBA-15 for esterifications. *J. Mol. Catal. A Chem.* **2007**, *271*, 46–56. [[CrossRef](#)]

33. Haider, M.H.; Dummer, N.F.; Zhang, D.; Miedziak, P.; Davies, T.E.; Taylor, S.H.; Willock, D.J.; Knight, D.W.; Chadwick, D.; Hutchings, G.J. Rubidium-and caesium-doped silicotungstic acid catalysts supported on alumina for the catalytic dehydration of glycerol to acrolein. *J. Catal.* **2012**, *286*, 206–213. [[CrossRef](#)]
34. Raveendra, G.; Rajasekhar, A.; Srinivas, M.; Prasad, P.S.S.; Lingaiah, N. Selective etherification of hydroxymethylfurfural to biofuel additives over Cs containing silicotungstic acid catalysts. *Appl. Catal. A Gen.* **2016**, *520*, 105–113. [[CrossRef](#)]
35. Sayenko, S.Y.; Shkuropatenko, V.A.; Dikiy, N.P.; Tarasov, R.V.T.; Ulybkina, K.A.; Surkov, O.Y.; Litvinenko, L.M. Clinoptilolite with Cesium Immobilization to Potassium Magnesium Phosphate Matrix. *East. Eur. J. Phys.* **2017**, *4*, 37–43. [[CrossRef](#)]
36. Kulikova, S.A.; Vinokurov, S.E. The Influence of Zeolite (Sokyrnytsya Deposit) on the Physical and Chemical Resistance of a Magnesium Potassium Phosphate Compound for the Immobilization of High-Level Waste. *Molecules* **2019**, *24*, 3421. [[CrossRef](#)] [[PubMed](#)]
37. Vinokurov, S.E.; Kulyako, Y.M.; Slyunchev, O.M.; Rovnyi, S.I.; Wagh, A.S.; Maloney, M.D.; Myasoedov, B.F. Magnesium potassium phosphate matrices for immobilization of high-level liquid wastes. *Radiochemistry* **2009**, *51*, 65–72. [[CrossRef](#)]
38. Vinokurov, S.E.; Kulikova, S.A.; Krupskaya, V.V.; Myasoedov, B.F. Magnesium Potassium Phosphate Compound for Radioactive Waste Immobilization: Phase Composition, Structure, and Physicochemical and Hydrolytic Durability. *Radiochemistry* **2018**, *60*, 70–78. [[CrossRef](#)]
39. Vinokurov, S.E.; Kulikova, S.A.; Krupskaya, V.V.; Tyupina, E.A. Effect of Characteristics of Magnesium Oxide Powder on Composition and Strength of Magnesium Potassium Phosphate Compound for Solidifying Radioactive Waste. *Russ. J. Appl. Chem.* **2019**, *92*, 490–497. [[CrossRef](#)]
40. GOST 310.4-81. *Cements. Methods of Bending and Compression Strength Determination*; Standardinform: Moscow, Russian, 1981; pp. 1–11.
41. GOST R 52126-2003. *Radioactive Waste. Long Time Leach Testing of Solidified Radioactive Waste Forms*; Standardinform: Moscow, Russian, 2003; pp. 1–8.
42. ANSI/ANS-16.1-1986. *Measurement of the Leachability of Solidified Low-Level Radiactive Wastes by a Short-Term Test Procedure*; American National Society: La Grande Park, IL, USA, 1986; pp. 1–30.
43. De Groot, G.; Van Der Sloot, H. Determination of Leaching Characteristics of Waste Materials Leading to Environmental Product Certification. In *Stabilization and Solidification of Hazardous, Radioactive, and Mixed Wastes*, 2nd ed.; ASTM International: West Conshohocken, PA, USA, 2009; p. 149.
44. Torras, J.; Buj-Corral, I.; Rovira, M.; De Pablo, J. Semi-dynamic leaching tests of nickel containing wastes stabilized/solidified with magnesium potassium phosphate cements. *J. Hazard. Mater.* **2011**, *186*, 1954–1960. [[CrossRef](#)]
45. Mimura, H.; Lehto, J.; Harjula, R. Chemical and Thermal Stability of Potassium Nickel Hexacyanoferrate (II). *J. Nucl. Sci. Technol.* **1997**, *34*, 582–587. [[CrossRef](#)]
46. Choi, J.; Um, W.; Choung, S. Development of iron phosphate ceramic waste form to immobilize radioactive waste solution. *J. Nucl. Mater.* **2014**, *452*, 16–23. [[CrossRef](#)]
47. Kim, M.; Kim, H.G.; Kim, S.; Yoon, J.-H.; Sung, J.Y.; Jin, J.S.; Lee, M.-H.; Kim, C.-W.; Heo, J.; Hong, K.-S. Leaching behaviors and mechanisms of vitrified forms for the low-level radioactive solid wastes. *J. Hazard. Mater.* **2020**, *384*, 121296. [[CrossRef](#)] [[PubMed](#)]

